Available online at www.sciencedirect.com
ScienceDirect
Biochimica et Biophysica Acta 1773 (2007) 912–923
Biochimica et Biophysica Acta
BBA
www.elsevier.com/locate/bbamcr

Relocalization of the polypyrimidine tract-binding protein during PKA-induced neurite growth

Shumei Ma, Guodong Liu, Yuan Sun, Jiuyong Xie *

Department of Physiology, Faculty of Medicine, University of Manitoba, 420 BMSB, 730 William Ave., Winnipeg, Canada MB R3E 3J7

Received 11 December 2006; received in revised form 7 February 2007; accepted 8 February 2007
Available online 22 February 2007

Abstract

Neurite RNA binding proteins are important for neurite growth, a process critical for neuronal development and regeneration after injury. It has been known that many RNA binding proteins undergo nucleocytoplasmic shuttling but how their nucleocytoplasmic distributions are regulated during neurite growth has not been well explored. Here we found that the polypyrimidine tract binding protein (PTB) was exported from the nucleus and accumulated at growing neurite terminals upon activation of the PKA pathway in PC12 cells in a PKA-target Ser16-dependent manner. RNA interference (RNAi) of PTB significantly disrupted the neurite growth. We then examined the role of cytoplasmic PTB in relation to mRNAs involved in neurite growth. We found that PTB was preferentially associated with the β-actin mRNA transcripts in cytoplasmic fractions. RNAi of PTB reduced neurite accumulation of the endogenous actin proteins. It is thus likely that, during PKA-induced neurite growth, PTB is relocalized through Ser16 phosphorylation to the cytoplasm where it is associated with β-actin mRNA and is critical for the mRNA localization to neurites.

Keywords: Polypyrimidine tract binding protein; PTB; PKA; Nucleocytoplasmic transport; Neurite growth; Phosphorylation; mRNA localization

1. Introduction

RNA binding proteins are important for the asymmetric distribution of mRNAs in cells from yeast to human [1]. In neurons, they are involved in mRNA localization and/or neurite growth [2–18]. For example, two RNA binding proteins ZBP1 and ZBP2 participate in the localization and translation of the β-actin mRNA through binding to the zipcode of the 3′ untranslated region (3′ UTR) [5,8,17–19]. Particularly, the ZBP1 protein has been shown to accompany the β-actin mRNA from the nucleus to the cytoplasm and the neurites, where the c-Src protein kinase phosphorylates the Tyr396 of ZBP1 for the actin mRNA to dissociate for translation. It has also been known that many mRNA binding proteins, including those that are mainly in the nucleus in the static state, shuttle between the nucleus and the cytoplasm [20,21]; and that disturbance of this process and the cytoplasmic localization of the proteins would affect neurite growth [22]. But there remains no direct molecular link between the nucleocytoplasmic distribution of RNA binding proteins and neurite-inducing signals.

PTB (hnRNP I) is a member of the heterogeneous nuclear ribonucleoprotein particle protein (hnRNP) family that are involved in many aspects of mRNA metabolism [20]. Several PTB genes have been identified including the commonly known PTB and nPTB [23–32]. PTB is expressed in neurons only during the embryonic stages and nPTB in both embryonic and adult neurons [33]. PTB protein represses alternative pre-mRNA splicing in the nucleus [23,34], and controls mRNA localization, stability and viral RNA translation in the cytoplasm [35–39], through binding to pyrimidine-rich sequences with a consensus of UUCU, UCUU or CUCU [23,34,40]. In a human embryonic kidney cell line, the nucleocytoplasmic distribution of PTB can be regulated by direct PKA phosphorylation of serine 16 (Ser16, Fig. 1a) [41], a critical residue in the nuclear localization and export signal domain [41–46]. Specifically, increased Ser16 phosphorylation relocalizes PTB from the nucleus to the cytoplasm [41]. In pancreatic beta cells, cytoplasmic PTB controls the stability of the insulin mRNA and the nucleocytoplasmic PTB relocalization is important for glucose-induced

* Corresponding author. Tel.: +1 204 975 7774; fax: +1 204 789 3934.
E-mail address: xiej@cc.umanitoba.ca (J. Xie).

0167-4889/$ - see front matter © 2007 Elsevier B.V. All rights reserved.
doi:10.1016/j.bbamcr.2007.02.006

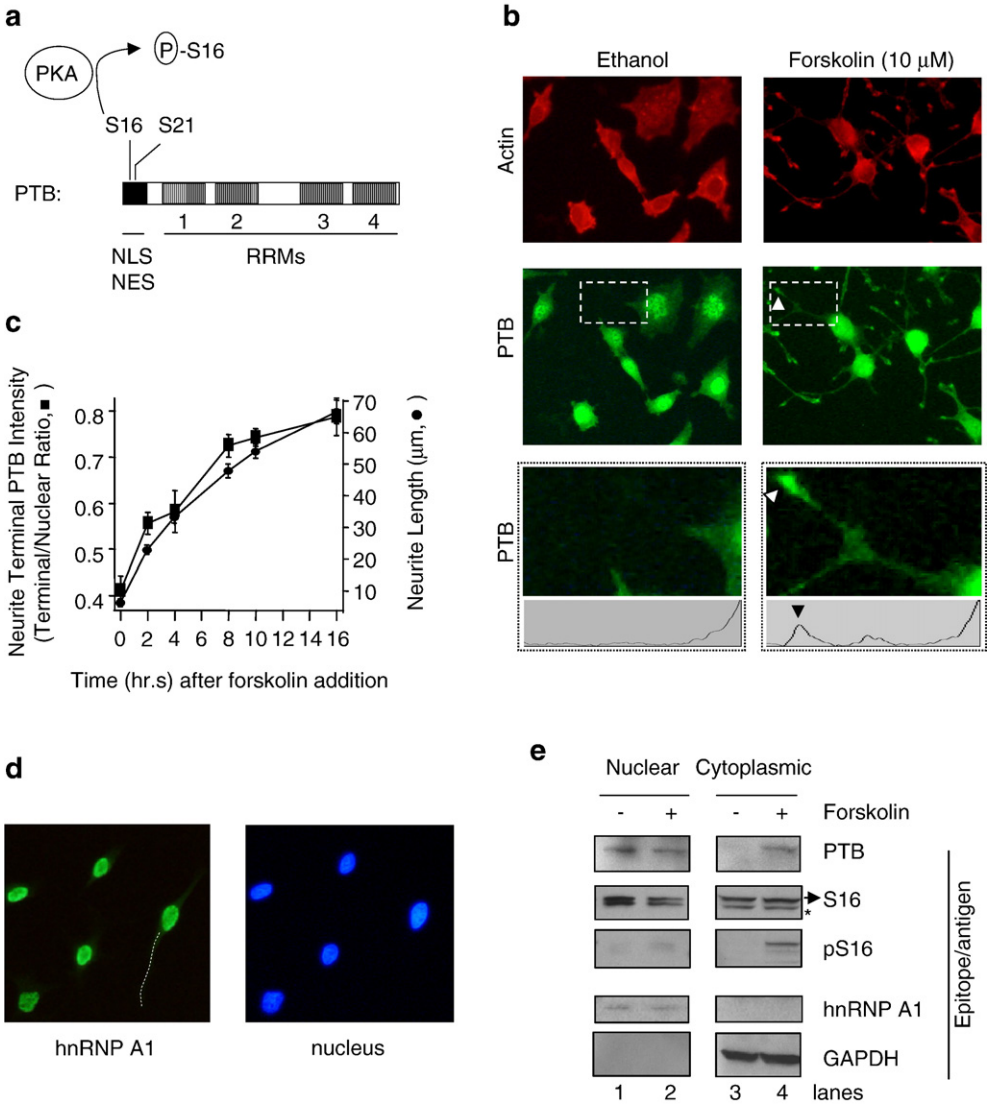

Fig. 1. Localization of PTB during forskolin-induced neurite growth. (a) Diagram of PTB phosphorylation by PKA in PC12 and other cells (Xie et al.). The black box represents the nuclear localization and export signal domain (NLS, NES) and boxes with vertical lines the four RNA recognition motifs (RRMs, not to scale). (b) Fluorescent images of PC12 cells treated for 8 h with either ethanol or forskolin (10 μM) and stained with either Phalloidin-TRITC (for actin, top panel) or anti-PTB antibody BB7 (middle and lower panels) as indicated above and to the left of the images. The bottom panel is an enlarged area outlined in the middle panel, with plots of PTB intensities in the neurites shown under the images. Note the presence of PTB immunoreactivity in the neurite terminals (green, and arrow-pointed) in the forskolin-treated cells (middle and lower panels). The secondary antibody used for the PTB staining is anti-mouse IgG-fluorescein. No fluorescent signals were seen without the primary antibody BB7. (c) Time course of the increase in immunoreactivity of neurite terminal PTB and neurite growth after forskolin addition (average±SEM). Neurite terminal PTB intensity was calculated as the ratio of neurite terminal to nuclear PTB intensity of the same-sized area of the same cells. For each cell, the longest neurite was measured as neurite length (same as in the following experiments). (d) Localization of the control protein hnRNP A1 (left) 8 h after forskolin addition. No neurite terminal or cytoplasmic enrichment of A1 protein was observed even under a brighter view. The dotted line in the left image aligns with the path of the neurite when observed under high contrast. Nuclei (stained with Hoechst 33250) of the same cells are shown to the right to verify the A1 localization in the nucleus. (e) Western blots of nuclear (lanes 1–2) or cytoplasmic (lanes 3–4) proteins from untreated (lanes 1,3) or forskolin-treated (lanes 2,4, for 4 h) PC12 cells with antibodies against endogenous PTB, nonphospho-Ser16 (S16, arrow-pointed) or the phospho-Ser16 (pS16) epitope of PTB. The lower band (∗) in the row of S16 is likely the nPTB which has a similar epitope as PTB (Xie et al.). The S16 signals are much stronger overall than PTB, likely due to differences in the affinity of the antibodies for these epitopes in rat samples. hnRNP A1 and GAPDH serve as C/N fractionation controls. Blots representative of 4 experiments.

insulin secretion [37,47–49]. In neuronal cells, whether the nucleocytoplasmic distribution of PTB changes and what is the role of cytoplasmic PTB during neurite growth remain unknown.

In neurons, the PKA pathway plays a critical role in inducing neurite growth and is required for mRNA localization in axon growth cones [19,50–53]. In rat pheochromocytoma PC12 cells, activation of the PKA pathway is sufficient to induce neurite growth [54,55]. Interestingly, phospho-Ser16-PTB is increased upon activation of PKA in PC12 cells [41]. Thus, PC12 cells offer an excellent system to study specifically the effect of the PKA pathway on PTB localization during neurite growth. Unfortunately, the PC12 cell strain used previously did not grow neurites efficiently and it is not clear whether the PTB localization in these cells was changed upon activation of the PKA pathway.

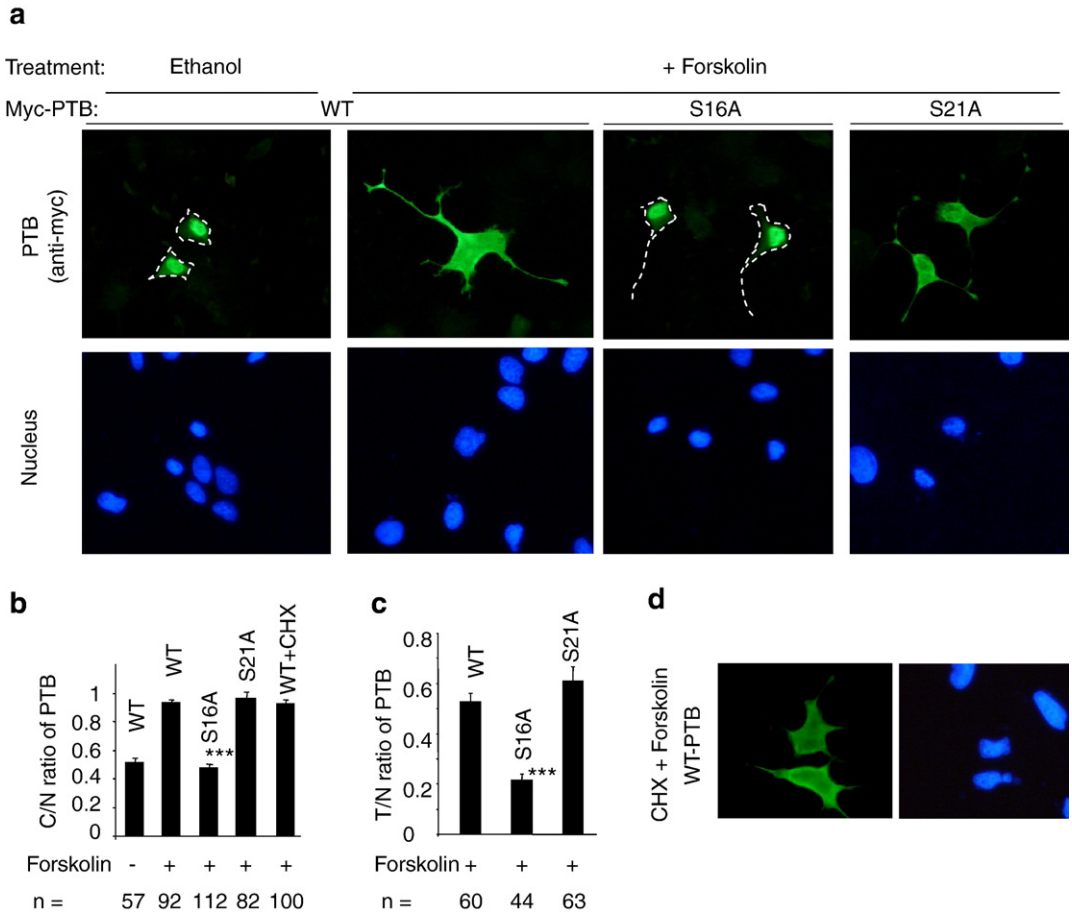

Fig. 2. Role of the PKA target Ser16 in PTB relocalization by forskolin. (a) Localization of wild type Myc-PTB (WT) and mutants (S16A and S21A) 8 h after ethanol or forskolin (10 μM) addition, as indicated above the images. Nuclear images of the same cells are shown below the Myc images. The neurite grown in the Myc-PTB S16A-transfected cells was verified by adjusting the image to brighter and high contrast views. The dotted lines indicate the cell edges or neurites under high contrast. (b) Average cytoplasmic to nuclear (C/N) Myc-PTB intensity ratios (±SEM) of the samples as in a (***$p<0.001$, in Student's *t*-test, same in the followings). C/N was taken as the ratio of cytoplasmic to nuclear PTB immunoreactivity of the same sized area of the same cells. (c) Average neurite terminal to nuclear (T/N) Myc-PTB intensity ratios (±SEM) of the samples as in a (***$p<0.001$). (d) Effect of cycloheximide on PTB relocalization by forskolin. Shown are immunostaining images of PTB (left) and nuclei (right) of PC12 cells treated with forskolin, with prior addition of cycloheximide (100 μg/ml).

In the present study, to characterize the localization and role of PTB during PKA-induced neurite growth, we used a PC12 strain that grew neurites efficiently upon activation of the PKA pathway [56], and examined the role of Ser16 in the nucleocytoplasmic distribution of PTB during PKA-induced neurite growth and cytoplasmic PTB's association with the mRNA essential for neurite growth.

2. Experimental methods

2.1. Cell culture and transfection

PC12 cells were cultured in Dulbecco's Modified Eagle's Medium (DMEM) with 10% horse serum plus 2.5% fetal bovine serum, at 37 °C with 5% CO_2. Transient transfection assays were carried out in 12-well plates (Falcon) using LipoFectamine 2000 (Invitrogen). Briefly, about 60% confluent PC12 cells of one 100 mm dish were resuspended and divided equally into each well of 12 well plates and incubated overnight. One and half micrograms of DNA were mixed with 3 μl of LipoFectamine 2000 in 50 μl of DMEM (serum- and antibiotics-free) and incubated at room temperature for 10 min. The mixture was then added to each well. For co-transfection with two plasmids, the volumes of lipid and DMEM were proportionally adjusted. After 3 h of incubation, the cells were supplied with fresh media and cultured for a period of time as specified in the text. Forskolin (10 μM) was dissolved in ethanol instead of DMSO, which induces growth of cell processes by itself (data not shown). In experiments with protein synthesis inhibitor, cycloheximide (100 μg/ml) was applied prior to the forskolin addition (Fig. 2d).

2.2. Immunostaining

Cover glasses (12 mm in diameter) were coated with poly-D-lysine (0.5 mg/ml, Sigma) at 4 °C overnight and put one into each well of 12 well plates. PC12 cells were plated over the coated cover glasses. Before staining, cells were rinsed in cold phosphate-buffered saline with 1% BSA, fixed with pre-chilled 4% PFA for 15 min and then permeabilized with 0.2% Triton-X 100 for 10 min at room temperature. The fixed cells were incubated overnight at 4 °C with primary antibodies, either mouse anti-PTB (BB7 [57], 1:200 dilution), rabbit anti-c-Myc (1:1000), or mouse anti-hnRNP A1 (1:1000). These cells were then washed and incubated with anti-mouse or anti-rabbit fluorescent secondary antibodies (1:1000, conjugated with Texas-Red for red colour or fluorescein for green colour) for 1 h at room temperature in the dark. Hoechst 33342 (1:5000) or Phalloidin-TRITC (1:10000) were used to highlight the nuclei or actin of cells in some experiments. Incubation and washes for the primary antibody were in TBS (20 mM Tris–Cl, 250 mM NaCl, plus 1% BSA) and for the secondary antibody in TBS without BSA. The stained cells were observed under fluorescent microscope (Nikon).

2.3. Cytoplasmic and nuclear fractionation and Western blot [41]

Briefly, for endogenous proteins, PBS (containing 1 mM EDTA) -washed cells grown in 100 mm plates were resuspended in 70 μl cold NP40 buffer [150 mM NaCl, 10 mM Tris (pH 7.8), 1 mM EDTA and 0.3% Igepal CA-630 (Sigma)] and spun down. The pellet was washed with PBS-EDTA, lysed in 140 μl RIPA buffer, sonicated and saved as nuclear fraction. The supernatant was layered onto a 24% sucrose cushion and spun at 14,000 rpm for 10 min at 4 °C, and then 90% of the upper layer above the sucrose was used as cytoplasmic fraction. For Western blotting of the PTB proteins, 20 μl of cytoplasmic or 10 μl of the nuclear fraction was loaded per lane. For Myc-PTB-transfected samples, two wells of cells grown in 6-well plates and transfected with plasmids (2 μg each) were similarly lysed and fractionated into 100 μl NP40 (C) or RIPA (N) buffer, and 10 to 15 μl was loaded per lane. The clean separation of cytoplasm (C) and nuclear (N) fractions was verified by the absence of hnRNP A1 and GAPDH proteins in the C and in the N fractions, respectively. Primary antibodies were incubated with 5% dry milk in TBS buffer containing 500 mM NaCl. Secondary antibodies were used at a dilution of 3000×. Final washes were in TBS containing 500 mM NaCl. The blots were then incubated with ECL reagents and exposed to X-ray films. Before reprobing, the blot membrane was incubated in stripping buffer (2% SDS, 100 mM β-mercaptoethanol, 50 mM Tris, pH 6.8) at 65 °C for 30 min.

2.4. Plasmid construction

Target sequences (sense, 5′→3′) of RNAi are chosen from the divergent 3′ UTR of mRNAs and cloned into pSilencer2.1-U6 neo (Ambion). The sequences tested are as follows (numberings are based on GenBank accession numbers X60789 for rat PTB [30] and AJ010585 for rat nPTB [27,28]): PTBi1680: TGACCTTACAGACCAGAG; PTBi2015 (PTBi): TCAAGTGACATGATT CTCC; PTBi2587: CGACTACAGGCTCAGTATT; PTBsm (scrambled PTBi): CTCCGAATACATTAGTGTC; PTBm (mutant of PTBi): TCAAGTctCAacAT TCTCC. nPTBi2230 (nPTBi): TTAACAAGATGCAGAGTAT; nPTBi2353: GTGTCAGCACTAAGTAATGT; nPTBi2841: GATTCATAGATTCTGTTAT. All sequences were blasted against the rat genome and no perfect matches with other genes were observed. They were cloned according to the plasmid supplier's protocol. Briefly, hairpin oligonucleotides were dissolved with sterile H_2O to 100 μM. Two microliters of each complementary oligonucleotide were mixed with 16 μl of annealing buffer (10 mM Tris–Cl, pH 7.5; 50 mM NaCl and 1 mM EDTA) and denatured at 95 °C for 5 min, followed by annealing at room temperature. The annealed oligonucleotides were phosphorylated (2 μl annealed oligonucleotide, 10 u T4 polynucleotide kinase, 0.1 mM ATP) at 37 °C for 30 min and then incubated at 70 °C for 10 min. The phosphorylated oligonucleotides were cloned between the *Hin*dIII and *Bam*HI sites of the pSilencer2.1-U6neo vector.

2.5. Gel mobility shift assay

The rat zipcode RNA probe was made by in vitro transcription from a T7-promoter tagged PCR product of reversed transcribed PC12 cell mRNAs. The full zipcode sequences used are: 5′-GCGGACUGUUACUGAGCUGC GUUUUACACCCUUUCUUUGACAAAACCUAACUUGCGCA-3′ (wild type) and 5′- GCGGACUGUUACUGAGCUGCGUUUUACACCCgUgaUgU GACAAAACCUAACUUGCGCA-3′ (mutant, mutated nucleotides in lower cases). Mutations were introduced with a mutant primer. Gel shift assay conditions are as reported by others [58], except that the interaction buffer was preincubated with 200 ng/μl of yeast tRNA and the complexes were resolved in a 4% native polyacrylamide gel.

2.6. Immunoprecipitation-RT-PCR

Three 150-mm dishes of PC12 cells treated with forskolin were lysed in NP40 cell fractionation buffer (600 μl total). A third of the cytoplasmic fraction was precleared with protein A-sepharose beads and added 2 μl antibody against PTB (BB7, ATCC) or hnRNP L (4D11, Santa Cruz), incubated with rocking at 4 °C for 1 h and washed in NP40 buffer with NaCl (300 mM final concentration). The resulting pellets were extracted for RNA with an RNA extraction kit (Sigma). About 40 ng RNA from the pellet and 400 ng from the supernatant were used in 10 μl reverse transcription reaction and 1 μl used in PCR (30 cycles for actin from supernatant and 40 cycles for the rest of the samples). PCR products were resolved in 3% agarose gel.

2.7. In vitro RNA transcription and probe labelling

Fluorescent UTP was incorporated into the zipcode RNA in in-vitro transcription reactions. Briefly, PCR fragments carrying a T7 promoter were purified by agarose gel electrophoresis and used as templates for in vitro transcription with T7 RNA polymerase. Reaction mixtures (100 μl containing 1× T7 transcription buffer, plus 1.5 mM ATP, 1.5 mM CTP, 1.5 mM GTP, 1.0 mM UTP, 0.02 mM fluorescein-12-UTP, 4 mM $MgCl_2$, 0.5 mM DTT, 500 ng DNA template and 10 μl T7 RNA polymerase) were incubated for 4–6 h at 37 °C, treated with 1u DNase for 30 min, followed by heating at 85 °C for 5 min. The fluorescent RNA probes were then purified by G-25 column. One hundred nanograms of labelled probes were transfected into PC12 cells using LipoFectamine 2000 according to the manufacturer's instructions (Invitrogen).

2.8. Image data analysis

The NIH Image J software (developed at the U.S. National Institutes of Health and available on the Internet at http://rsb.info.nih.gov/ij/) was used to measure the immunofluorescence intensity. Same sized circle areas were measured from neurite terminal (T), cytoplasm (C) or nucleus (N) of each cell to obtain intensity ratios of T/N or C/N. To measure neurite length, the EGFP or actin images were adjusted to high contrast for a clear view of the neurites. The longest neurite was measured for each cell's neurite length. For the RNA interference groups, acquiring images and measurement of the neurite lengths were carried out with double blind test, where the cover slips prior to imaging were shuffled in a 12-well plate and identity kept by another person.

2.9. Statistical analysis

The statistical significance of differences between samples was tested with two-tailed Student's *t*-test.

3. Results

3.1. PTB relocalizes to the cytoplasm and neurite terminals upon activation of the protein kinase A pathway

To examine the localization of PTB in PKA-mediated neurite growth, we obtained a PC12 strain that grew neurites efficiently in response to forsklin or cAMP treatment [56]. In this cell line, both PTB and nPTB proteins are expressed. Here we will focus on the PTB protein since its expression in neurons is restricted to the embryonic stage [33], and mention briefly our data on nPTB in comparison with PTB.

In untreated or ethanol-treated PC12 cells, neurite growth was rare and PTB was mainly in the nucleus (Fig. 1b and e). In cells treated with forskolin, a well known activator of the adenylate cyclase of the PKA pathway [59], neurites grew to an average length of 48 μm (±2.24 μm, average±SEM, $n=25$ cells, Fig. 1b and c) within 8 h. Similar results were obtained by treatment with a cyclic AMP analogue cpt-cAMP. Moreover, the forskolin-induced neurite growth was disrupted by a PKA inhibitor KT5720 (data not shown). Most strikingly, the neurite terminals were enriched with PTB immunoreactivity in these cells. The ratio of the neurite terminal to nuclear PTB intensity (T/N) increases during the outgrowth of neurites (Fig. 1c). This

was accompanied by a more homogeneous distribution of PTB in the cell soma and a 15% increase of the cytoplasmic to nuclear PTB intensity ratio (C/N). In contrast, hnRNP A1, another shuttling hnRNP protein that is mainly nuclear without forskolin treatment, still remained in the nucleus and was not increased in the cytoplasm or enriched at the neurite terminals after treatment (Fig. 1d). Therefore, the increased cytoplasmic and neurite localization is specific for the PTB protein rather than a general effect by forskolin on nuclear factors.

The nPTB protein, mainly cytoplasmic before treatment, also localized to the neurite terminals but with no obvious changes in its nucleocytoplasmic distribution upon forskolin treatment (data not shown).

To verify the relocalization of PTB protein and its phosphorylation status (phospho-Ser16-PTB) during forskolin induction, we probed Western blots of cytoplasmic and nuclear fractions of PC12 cells treated with forskolin, using antibodies specific for PTB (BB7, recognizing both nonphospho- and phospho- Ser16-PTB) [41,57], nonphospho-Ser16-PTB (S16), phospho-Ser16-PTB (pS16), or hnRNP A1 (Fig. 1e). Similar to the immunostaining result in Fig. 1b, PTB is clearly detectable with the BB7 antibody in the nucleus but not the cytoplasm without forskolin treatment (Fig. 1e, lanes 1 and 3). The nuclear PTB decreased and the cytoplasmic PTB was increased upon forskolin treatment (lanes 2 and 4). The anti-S16 antibody gave much stronger signals making the cytoplasmic PTB detectable even in the non-forskolin sample (lane 3). The nonphospho-Ser16-PTB (S16) was decreased in the nucleus but not increased comparably in the cytoplasm upon forskolin treatment. The phospho-Ser16-PTB (pS16) was invisible in both fractions when no forskolin was added (lanes 1 and 3), but clearly detected and mainly in the cytoplasmic fraction upon forskolin treatment (lanes 2 and 4). In contrast, the hnRNP A1 protein band was neither increased in the cytoplasm nor decreased in the nucleus by forskolin treatment. Thus, the Western blot data is consistent with the observed PTB relocalization from nucleus to the cytoplasm by immunostaining (Fig. 1b). Moreover, phospho-Ser16-PTB is sharply increased in the cytoplasm upon forskolin treatment, supporting that PKA phosphorylation of PTB is involved in its relocalization from the nucleus to the cytoplasm.

3.2. The PKA target S16 is required for PTB relocalization during neurite growth

To confirm the involvement of the PKA pathway and its target Ser16 in the PTB relocalization to both the cytoplasm and neurite terminals upon forskolin treatment, we then examined the effect of Ser16 mutation on the localization of PTB, with the previously tested Myc-tagged wild type PTB (WT), the S16A (serine 16 changed to alanine) or the S21A (serine 21 changed to alanine) mutant [41].

The wild type Myc-PTB was mainly in the nucleus when cells were not treated or treated with ethanol, with an average C/N (cytoplasmic to nuclear Myc-PTB intensity) ratio of 0.51 (±0.03, $n=57$ cells, Fig. 2a and b). Forskolin treatment relocalized a substantial amount of Myc-PTB to the cytoplasm within 8 h (C/N ratio: 0.93±0.02, $n=92$ cells). Moreover, these cells grew neurites similarly as those transfected with the control plasmid expressing the enhanced green fluorescent protein (EGFP) and more than half (57%, $n=47$ cells) of them contained enriched Myc-PTB at neurite terminals, with an average T/N ratio of 0.53 (±0.03, $n=60$ cells). In contrast, the S16A mutant remained mostly nuclear upon forskolin treatment, with a C/N ratio close to the ethanol-treated wild type samples (Fig. 2a and b), although these cells still grew out neurites as verified under brighter views. Moreover, the presence of the S16A mutant protein at neurite terminals was reduced to an average T/N ratio of 0.22 (±0.03, $n=44$ cells). Both the C/N and T/N ratios of the S16A are significantly lower than the WT samples (Fig. 2b and c). In comparison, the control mutant S21A was similarly relocalized by forskolin as the wild type Myc-PTB. Therefore, the S16A mutation specifically abolishes the Myc-PTB relocalization to the cytoplasm and the neurites in response to forskolin induction. This indicates that the Ser16 phosphorylation is essential for PTB to relocalize from the nucleus to the cytoplasm and neurite terminals.

The forskolin-induced Myc-PTB relocalization to the cytoplasm was not affected by prior application of the protein synthesis inhibitor cycloheximide (Fig. 2b and d), though the growth of neurites was drastically disrupted. This suggests that the cytoplasmic Myc-PTB proteins are mostly exported from the nucleus rather than newly synthesized after forskolin addition.

3.3. RNA interference of PTB disrupts neurite growth

Neurite RNA binding proteins and associated mRNAs have been implicated in neurite growth. The relocalization of PTB to the neurite terminals by PKA during PKA-induced neurite growth implies that PTB plays a role at the growing neurite terminals. We are also aware that the overexpression of Myc-PTB or its mutants did not affect neurite growth (Fig. 2a); however, overexpressed PTB may exert complex effects not seen by endogenous PTB. Therefore, to determine whether endogenous PTB plays a role in the PKA-mediated neurite growth, we carried out RNA interference assays against the expression of PTB.

We first tested PTB sequences as short hairpin RNAs expressed from silencer plasmids [60]. To visualize the hairpin RNA-expressing cells, we co-transfected each silencer plasmid with an EGFP plasmid (Silencer:EGFP=2:1) and the RNAi effect was monitored 3 days later by immunostaining of PTB in comparison with the non-EGFP cells in the same images. Co-transfection of one silencer PTBi2015 (called PTBi hereafter) with EGFP consistently reduced endogenous PTB immunoreactivity (up to 60% reduction, average 45±3%, Fig. 3), compared to the non-EGFP cells in the same images. In contrast, transfection of the EGFP plasmid alone did not reduce the PTB immunoreactivity (100±4% of non-EGFP cells in the same images, $n=13$); neither did the PTBi control plasmids PTBsm (with scrambled PTBi sequence) and PTBm (with 4 nucleotide mismatches from the PTBi sequence).

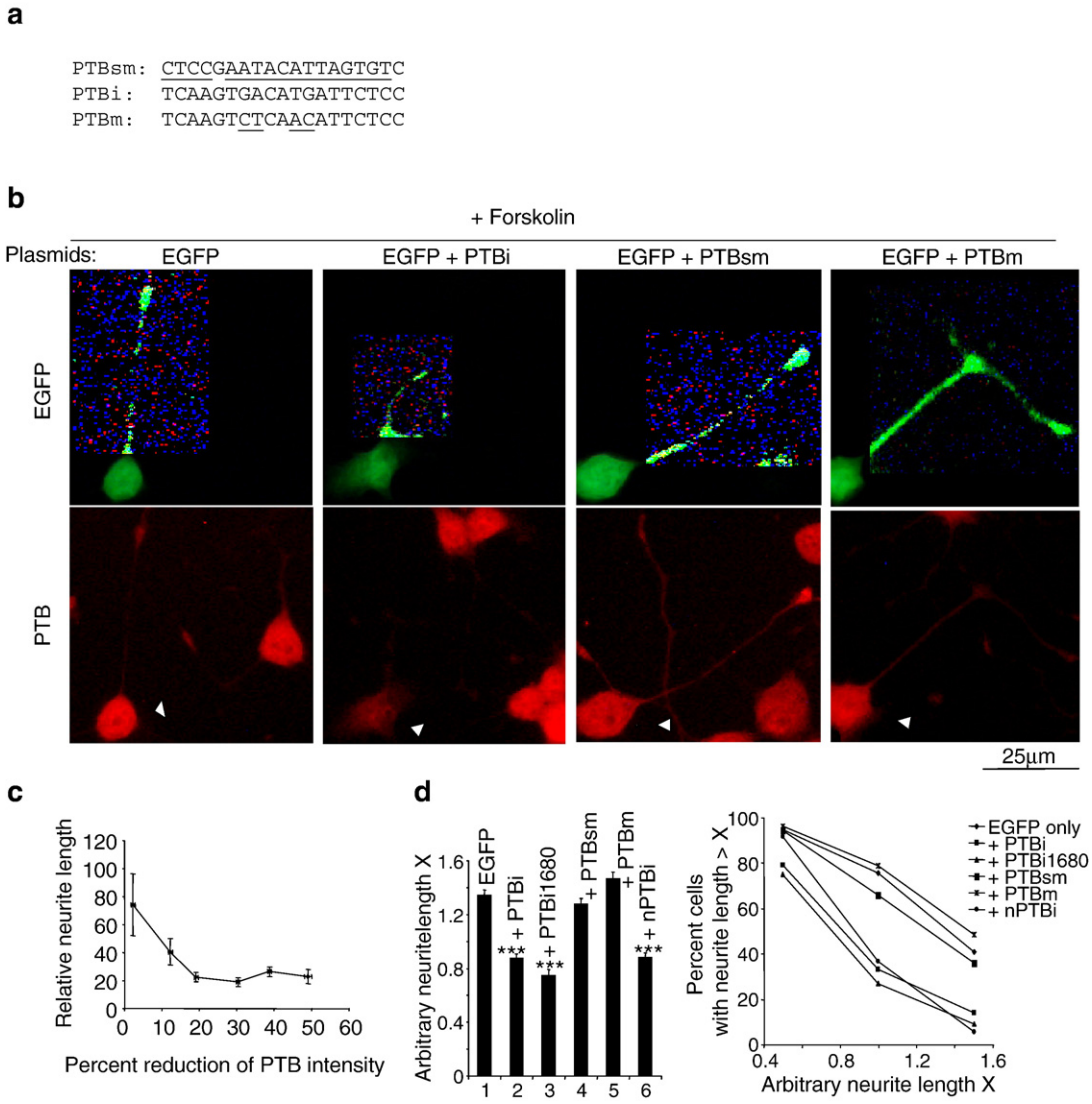

Fig. 3. Effect of PTB RNAi on forskolin-induced neurite growth. (a) Target sequences used for the PTBi, PTBsm and PTBm plasmids as indicated to the left. Nucleotides different from the wild type PTB sequence are underlined. (b) Neurite growth of PC12 cells transfected with EGFP alone (left column), EGFP plus PTBi (second column from left) or plus PTBsm (with scrambled PTBi sequence, third from left), or plus PTBm (with 4 nt mismatches from the PTBi sequence, fourth from left) for 3 days, and then induced with forskolin for 8 h. Shown are EGFP (green, upper) or PTB (red, lower) images for the same views of each treatment group. The arrowheads point to the corresponding EGFP-positive cells in the upper panel. The longest neurites (processes) in each image are highlighted with high-contrast areas. (c) Neurite length decreases with reduced PTB intensity. The length and PTB intensity are relative to that of the non-EGFP cells with the highest PTB intensity in the same images (from left to right: $n=4$, 12, 26, 38, 34, 9 cells for each point). (d) Left, average neurite length index X (X, arbitrary unit, ± SEM) of cells transfected with silencer (columns 2, 3, 6) or control (columns 1, 4, 5) plasmids. ***$p<0.001$, compared to the group transfected with EGFP only. $N=216$, 254,135, 246, 155 and 129 cells for columns 1–6, respectively. Right, percent distribution of neurites longer than a given length in the different groups. Result of nPTBi samples is also included. The longest neurite was measured for each cell. Imaging and measurement of the neurites were carried out with double blind tests as described in Experimental methods. These data were from 3 experiments.

After transfection of EGFP alone or EGFP with the silencer PTBi or control plasmids for 3 days, we treated the cells with forskolin for 8 h and then measured the neurite length. In cells transfected with EGFP alone, neurites still grew well (Fig. 3b and d, arbitrary neurite length index: 1.34±0.04, $n=216$). In contrast, in most cells co-transfected with EGFP and PTBi, only very short protrusions grew out (index: 0.88±0.03, $n=254$). Moreover, in these cells, neurite length decreased with reduced PTB intensity (Fig. 3c). In contrast, cells co-transfected with control plasmids PTBsm or PTBm grew neurites efficiently (index: 1.28±0.04, $n=246$, and 1.46±0.05, $n=155$ respectively). Thus, the average neurite length of the PTBi group is significantly shorter than that of the control groups.

The percent distribution of neurite length among the RNAi and control groups also indicates that the PTBi group has generally much shorter neurites than the others (Fig. 3d, right). For example, in the PTBi group less than 30% cells grew neurites with a length index number higher than 1.0 while in the other groups there were more than 60% cells.

To further support the specificity of the PTBi effect on neurite growth, another PTB silencer PTBi1680, targeting a

different sequence of PTB 3′ UTR, disrupted neurite growth similarly (Fig. 3d).

Taken together, these results demonstrate that interference with the expression of the PTB protein disrupts neurite growth induced by the PKA pathway.

Interestingly, we noticed that the RNAi knockdown of nPTB also reduced the PKA-induced neurite growth (Fig. 3d, and see below and Discussion).

3.4. Association of cytoplasmic PTB with β-actin mRNA

Among others, one possibility for the disrupted neurite growth is a disrupted cytoplasmic function of PTB by PTBi. We then looked for potential PTB binding sites among the known 3′ UTR RNA elements of genes involved in neurite growth or elements sufficient to mediate neurite localization of mRNAs. We noticed the known consensus PTB binding sequences UUCU and CUCU in at least four mammalian mRNAs: GAP-43 [61], Tau [62], CaMK IIα [63] and β-actin [64] (Fig. 4). Particularly β-actin has been known to be involved in axon growth and its mRNA localization to the growth cone is stimulated by forskolin or db-cAMP [8,19,65]. The mammalian β-actin neurite localization signal (called zipcode) sequence harbours a pyrimidine-rich sequence containing UUCU (Fig. 4), different from that in the chick zipcode [64]. Preliminary tests with a rat zipcode RNA probe detected a weak but consistent and UUCU-dependent interaction with PTB in gel mobility shift assays (Fig. 5a). Therefore, we focused on β-actin as an example of neurite mRNA in association with cytoplasmic PTB.

We first examined the association between the endogenous β-actin mRNA and PTB in the cytoplasmic fractions of forskolin-treated PC12 cells by immunoprecipitation with anti-PTB antibody followed by RNA extraction from the supernatant or pellet and then RT-PCR, similarly as done for other proteins [5]. Beta-actin was preferentially amplified from pellet RNA samples immunoprecipitated by the PTB but not the hnRNP L antibody (Fig. 5a, lanes 4–6, upper gel). In contrast, GAPDH was not amplified in any of the IP pellets (lanes 4–6, bottom gel). Thus, the cytoplasmic PTB protein is preferentially associated with the β-actin mRNA transcript.

To test whether mutation of the potential PTB binding site would affect the zipcode RNA localization to neurites, we transfected fluorescein-labelled rat zipcode wild type or mutant RNAs into PC12 cells and examined their localization upon forskolin induction (Fig. 5b). To avoid drastic interruption of the ZBP1 binding, the pyrimidine-rich motif in the wild type RNA was replaced in the mutant with the corresponding chick

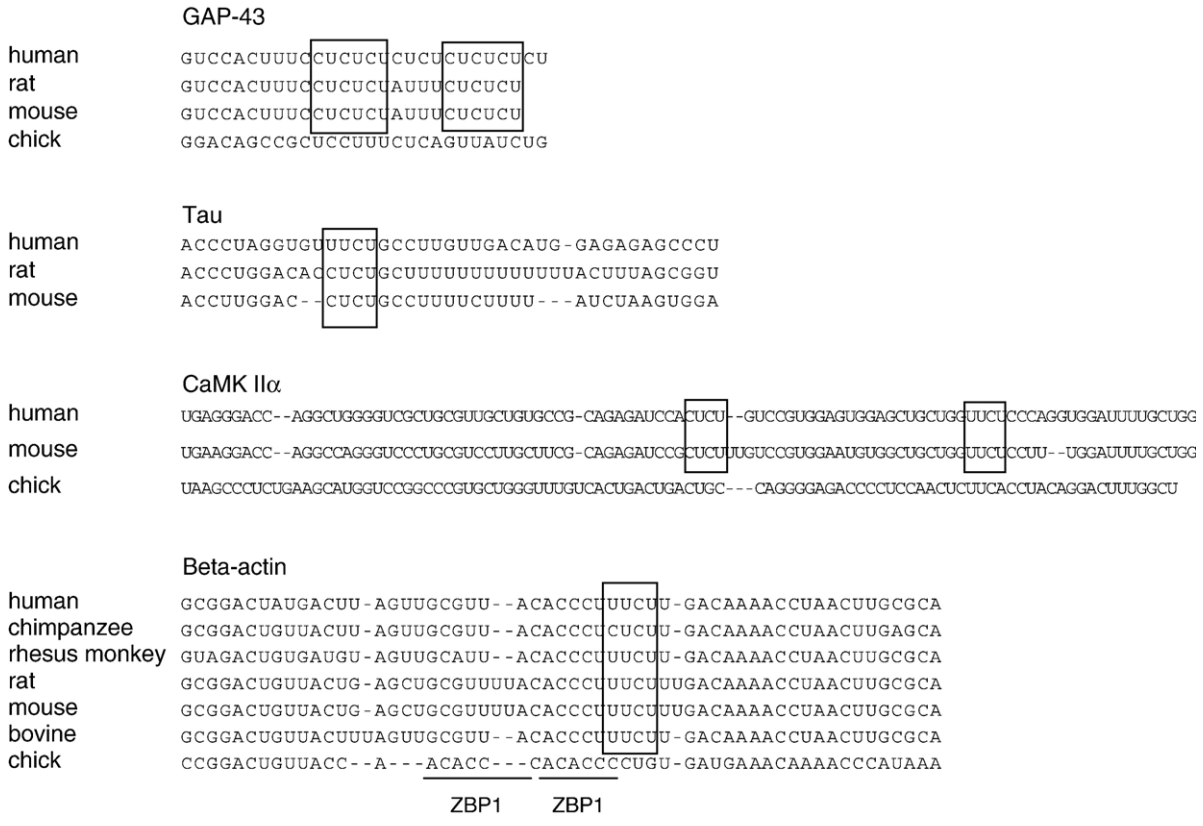

Fig. 4. Potential PTB binding sites in the stability control region rbr1 of the GAP-43 mRNA and in neurite localization signals of other mammalian mRNAs. The sequences of GAP-43, Tau, CaMK IIα, and β-actin from several species (wherever available, indicated to the left of each sequence) are shown under the respective names. Boxed are the consensus PTB target motifs in mammals. The underlined beta-actin sequences (ACACCC) are ZBP1 binding motifs. The beta-actin regions corresponding to the chicken zipcode are from sequences with GenBank accession numbers NM_001101 (human), NM_031144 (rat), NM_007393 (mouse), AY141970 (bovine) and NM_205518 (chick). The sequences for chimpanzee and monkey are obtained using UCSC BLAT search in the respective genome database (http://www.genome.ucsc.edu/cgi-bin/hgBlat).

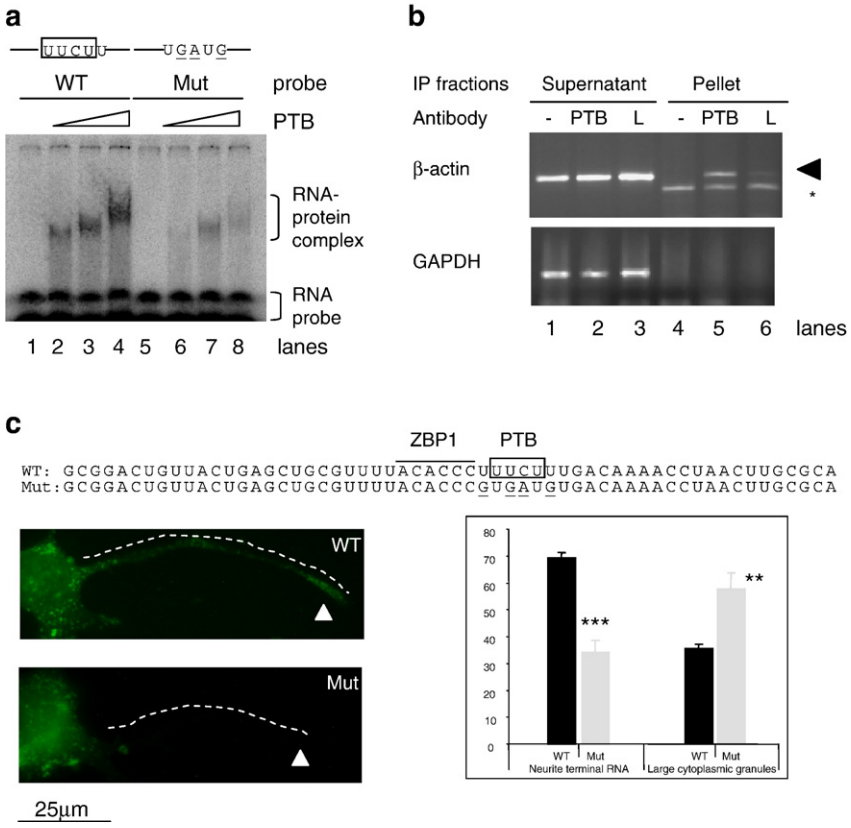

Fig. 5. Association of cytoplasmic PTB with β-actin mRNA transcripts. (a) Gel mobility shift assay of the interaction of PTB and zipcode RNA wild type (WT) or mutant (Mut) probes. PTB concentrations are 0, 200, 400 and 800 nM from left to right for each probe (~10 fmol). Mutated sequence region in the probe is indicated (not to scale) with the UUCU boxed and mutated nucleotides underlined. Gel representative of 3 experiments. (b) An agarose gel of the RT-PCR products of β-actin (upper) and GAPDH mRNA (lower) extracted from supernatant (lanes 1–3) or pellet (lanes 4–6) of immunoprecipitated cytoplasmic lysates of PC12 cells pre-treated with forskolin. The antibodies used for immunoprecipitation are for PTB or hnRNP L (L, as control) as indicated above the upper gel. The arrowhead indicates the actin product and the asterisk a non-specific product. Similar results were obtained from three experiments. (c) Localization of in vitro transcribed (fluorescein-UTP-labelled) wild type (WT) β-actin zipcode RNA and a mutant of the potential PTB binding site (Mut) in forskolin treated PC12 cells. The wild type and mutant zipcode RNA sequences are shown on top with the mutated nucleotides underlined. The UUCU motif is boxed and the ZBP1 binding motif ACACCC is marked with a line above. Note that the mutated nucleotides are chosen from the chick zipcode sequence in Fig. 4. The fluorescent images of neurite zipcode RNA are shown below to the left, with the dotted lines aligning above the neurites. To the right is a graph of the relative percentages (average±S.D., $n=3$ experiments) of cells with enrichment of zipcode RNA at the neurite terminals or with large cytoplasmic RNA granules (>1.25 μm in diameter) of the WT (solid black bars) and Mut (gray bars) RNA. $^{**}p<0.01$, $^{***}p<0.001$.

non-pyrimidine-rich sequence [66]. The wildtype RNA appeared as granules in both the cytoplasm and neurite terminals (Fig. 5c). Its enrichment in neurite terminals was found in about 70% of cells. In contrast, enrichment of the mutant RNA at neurite terminals was found in only about 35% of cells. Examination of their cytoplasmic granules indicates that mutant RNAs formed more large granules (>1.25 μm in diameter) than the wild type. The percentages of cells containing large cytoplasmic granules are about 35% and 60% for the wild type and mutant, respectively. The mutation thus appears to reduce zipcode RNA enrichment at the neurite terminals and this is accompanied by the presence of more large granules inside the cytoplasm. Therefore, the UUCU sequence region is critical for the zipcode RNA localization to neurite terminals.

Taken together, these results suggest that the cytoplasmic PTB is associated with the β-actin mRNA transcripts and is essential for their localization to neurite terminals.

To test whether interference of the PTB protein expression by RNAi affects the localization of β-actin protein to neurites, we examined the localization of β-actin protein in PTBi-treated cells by immunostaining. Neurite terminal accumulation of beta actin protein is significantly reduced in PTBi cells compared to others. The relative immunoreactivity of the beta-actin protein at neurite terminals (compared to that in the middle of the neurites) is reduced from 3.5 (±1.3, $n=4$) in cells cotransfected with PTBsm to 0.8 (±0.3, $n=4$, $p<0.01$) in cells transfected with the PTBi plasmid. Percentage of cells with enriched β-actin proteins at the neurite terminals was consistently reduced in the PTBi group (about 44% reduction) compared to that in the control groups (Fig. 6). PTB is thus required for the enrichment of β-actin protein at neurite terminals.

The nPTBi cells have reduced actin protein at the neurite terminals as well (Fig. 6b).

Overall, taking advantage of the PC12 cell neurite growth model with a specific signalling pathway, we show that during

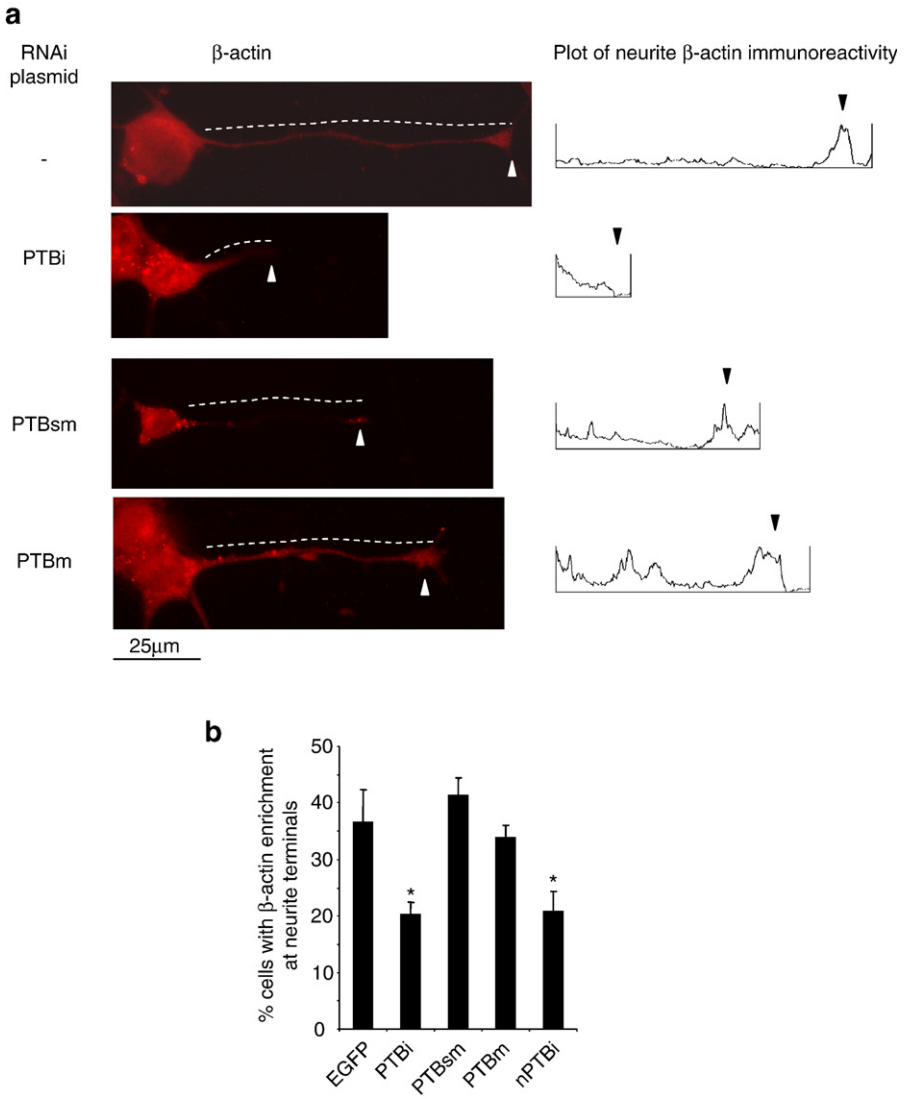

Fig. 6. The effect of PTBi on the localization of β-actin protein in forskolin-induced cells. (a) Representative fluorescent images (Red) of PC12 cells expressing EGFP, or EGFP plus PTBi, PTBsm or PTBm plasmids (indicated to the left of each image) and immunostained with anti-β-actin antibody and Texas-Red-conjugated secondary antibody. Intensity plots of neurite β-actin protein immunoreactivity are shown to the right of each image; the dotted lines align with the neurites and the neurite terminals are indicated with arrowheads. (b) Bar graph of the percentage (average±S.D., $n=3$ experiments) of cells (>250 cells each group) with neurite enrichment of β-actin protein immunoreactivity in the cells in a. Result for the nPTBi cells is also included (at the right). *$p<0.05$, compared to the EGFP group.

PKA induced neurite growth, PTB is exported out of the nucleus and accumulated in a Ser16-dependent manner in the cytoplasm, where it is associated with specific mRNA transcripts and is critical for their localization to the neurite terminals. This is likely at least one way for PTB to control neurite growth.

4. Discussion

RNA localization and RNA binding proteins are known involved in neurite growth [2]. Many RNA binding proteins are multifunctional in both the nucleus and cytoplasm and their distribution can be controlled through nucleocytoplasmic shuttling [20,21]. It has not been clear how the nucleocytoplasmic distribution of RNA binding proteins is regulated by neurite-inducing signals during neurite growth and their roles in the cytoplasm. In the present study, we examined the localization of PTB during PKA-induced neurite growth and its association with cytoplasmic mRNA transcripts essential for neurite growth, and show that the Ser16 of PTB is critical for its relocalization to the cytoplasm and neurites upon PKA activation during neurite growth. The cytoplasmic PTB is preferentially associated with the β-actin mRNA and PTB reduction by RNAi affects actin protein localization to the neurite terminals. Without excluding the role of nuclear PTB in mRNA processing [23,67–69], these data suggest that shift of the nucleocytoplasmic distribution of PTB likely plays a role in the localization of target neurite mRNAs during PKA-induced neurite growth.

In the cytoplasm, PTB regulates mRNA localization or stability through binding to the pyrimidine-rich elements of the 3′ UTR [35,38,47,70]. Particularly relevant to neurite growth is

the binding of a PTB protein (nPTB) to the mRNA stabilization rbr1 region of the growth-associated protein-43 (GAP-43) mRNA upon NGF stimulation of PC12 cells [61]. Thus, stabilization of the GAP-43 mRNA by nPTB, possibly PTB as well, could be one way for them to contribute to neurite growth; however, this does not explain why PTB needs to be localized to the neurite terminals during neurite growth.

To explore the role of PTB in association with a cytoplasmic mRNA known to be localized in neurites during neurite growth, we took β-actin mRNA as an example to investigate. Beta-actin mRNA localization has been known to be essential for cell motility and neuronal axon growth [18]. Our results indicate that PTB is associated with the β-actin mRNA in the cytoplasm (Fig. 5). Taken together with the reduced neurite localization of the zipcode mutant RNA (Fig. 5b), it is likely that PTB is involved in the actin mRNA localization to neurites.

Cytoplasmic PTB is known to control the localization or metabolism of several other RNA transcripts, including the Vg1 mRNA in *Xenopus* oocytes [35], viral RNAs [39,71], insulin mRNA in pancreatic beta cells [47,49], and CD154 mRNA in immune cells [38]. In the case of insulin mRNA, glucose-induced PTB relocalization to the cytoplasm through Ser16 phosphorylation stabilizes the insulin mRNA and upregulates the biogenesis of insulin granules [47]. PTB may also control GAP-43 mRNA stability during neurite growth [61], considering the similarity between the target sequences of PTB and nPTB. The mammalian Tau mRNA also contains the consensus PTB binding site in its neurite localization signal (Fig. 4). A recent large scale analysis in HeLa cells indicates that PTB-associated transcripts are enriched in mRNA species that encode proteins implicated in intracellular transport, vesicle trafficking and apoptosis [72]. Therefore, the cytoplasmic PTB is likely associated with a diverse group of mRNAs to control their localization or metabolism to regulate cell/virus functions during development, in viral infection, in endocrine secretion, immune response and neurite growth. It will be interesting to characterize these and other mRNAs that are associated with PTB to determine the role of cytoplasmic PTB in cell functions. The shift of the nucleocytoplasmic distribution of PTB controlled by cell signalling likely represents a common theme for PTB to function appropriately in both the nucleus and cytoplasm according to cell's physiological requirements.

With diverse mRNA targets of PTB in the cytoplasm identified and the regulated nucleocytoplasmic distribution of PTB shown, one may wonder where inside a cell these target mRNAs start to be associated with PTB. In the case of ZBP1, the beta-actin mRNA is accompanied by ZBP1 in the nucleus to the cytoplasm and neurites [17]. It has been known that some splicing factors in the nucleus deposit in the exon–exon junction (EJC) complex and accompany the mRNA to export to the cytoplasm [73]. Interestingly a recent report suggests that nuclear PTB likely facilitates the export of spliced HIV-1 RNA transcripts and increase their accumulation in the cytoplasm to reverse viral latency [39]. However, there is also a report demonstrating that the nuclear export of PTB is uncoupled from mRNA synthesis [45]. Thus, it remains unclear where the PTB target cytoplasmic mRNAs start to be associated with PTB and whether PTB deposits in the EJC complex after splicing to accompany RNA to the cytoplasm.

Other inducers such as NGF also induce neurite growth in PC12 cells but involving more complex signalling pathways [74]. We did not observe an effect for PTBi on NGF-induced neurite growth in an experiment with the PC12 cells (Ma and Xie, unpublished observation). Whether the PTBi effect on neurite growth in PC12 cells is limited to the PKA pathway is an interesting question for further investigation.

PTB and nPTB have similar binding sequences but can have different functions in other assays [24]. Unlike Myc-PTB overexpression (Fig. 2a and related text), nPTB overexpression suppresses neurite growth in PC12 cells [27]. Moreover, RNA interference of either PTB or nPTB disrupts forskolin-induced neurite growth (Fig. 3d), indicating that during neurite growth they have non-complementary functions, in addition to their both involvement in β-actin protein localization in the PKA-induced neurite growth. It will be interesting to know what these functions are and the underlying molecular basis.

In summary, using the PC12 cell model system with a well-known specific PKA pathway sufficient to induce neurite growth, we show that PTB, a primarily nuclear RNA binding protein, is relocalized to the cytoplasm and neurite terminals during PKA-induced neurite growth. This relocalization is mediated by PKA phosphorylation of Ser16. Moreover, the cytoplasmic PTB is associated with β-actin mRNA and reduction of PTB by RNAi affects the β-actin protein localization to neurites and PKA-induced neurite growth. This provides an inducible system for tracking down and studying the molecular details of an RNA binding protein, along its path from the nucleus to neurite terminals during neurite outgrowth. Studying these dynamic processes will provide insights into the molecular basis of neurite growth control by localized mRNA and RNA binding proteins and will be helpful for us to understand neurite growth during brain development and repair of neurons after injury.

Acknowledgements

We thank Jim Nagy for PC12 cells, Etienne Leygue, Doug Black, Robert Shiu, Qiang Wu, Jim Nagy, Angus Nairn, Yaling Zhou, Wenguang Cao, Mansoreh Nazari, Jiming Kong, Amy Pandya, Geetanjali Chawla, Ivan Babic, Peter Cattini, Janice Dodd and Mary Lynn Duckworth for their help or critical comments. We are grateful to Doug Black for plasmids and antibodies. Supported to J.X. by the Manitoba Medical Service Foundation, Manitoba Health Research Council and in part by the Canadian Institutes of Health Research (CIHR). J.X. is a CIHR New Investigator and a recipient of CFI fund.

References

[1] C.L. de Hoog, L.J. Foster, M. Mann, RNA and RNA binding proteins participate in early stages of cell spreading through spreading initiation centers, Cell 117 (2004) 649–662.
[2] O. Steward, Translating axon guidance cues, Cell 110 (2002) 537–540.
[3] O. Steward, mRNA localization in neurons: a multipurpose mechanism? Neuron 18 (1997) 9–12.

[4] S.J. Tang, D. Meulemans, L. Vazquez, N. Colaco, E. Schuman, A role for a rat homolog of staufen in the transport of RNA to neuronal dendrites, Neuron 32 (2001) 463–475.
[5] W. Gu, F. Pan, H. Zhang, G.J. Bassell, R.H. Singer, A predominantly nuclear protein affecting cytoplasmic localization of beta-actin mRNA in fibroblasts and neurons, J. Cell Biol. 156 (2002) 41–51.
[6] H.L. Zhang, T. Eom, Y. Oleynikov, S.M. Shenoy, D.A. Liebelt, J.B. Dictenberg, R.H. Singer, G.J. Bassell, Neurotrophin-induced transport of a beta-actin mRNP complex increases beta-actin levels and stimulates growth cone motility, Neuron 31 (2001) 261–275.
[7] B. Ye, C. Petritsch, I.E. Clark, E.R. Gavis, L.Y. Jan, Y.N. Jan, Nanos and Pumilio are essential for dendrite morphogenesis in *Drosophila* peripheral neurons, Curr. Biol. 14 (2004) 314–321.
[8] D.M. Tiruchinapalli, Y. Oleynikov, S. Kelic, S.M. Shenoy, A. Hartley, P.K. Stanton, R.H. Singer, G.J. Bassell, Activity-dependent trafficking and dynamic localization of zipcode binding protein 1 and beta-actin mRNA in dendrites and spines of hippocampal neurons, J. Neurosci. 23 (2003) 3251–3261.
[9] P.B. Crino, J. Eberwine, Molecular characterization of the dendritic growth cone: regulated mRNA transport and local protein synthesis, Neuron 17 (1996) 1173–1187.
[10] P. Litman, J. Barg, L. Rindzoonski, I. Ginzburg, Subcellular localization of tau mRNA in differentiating neuronal cell culture: implications for neuronal polarity, Neuron 10 (1993) 627–638.
[11] S. Layalle, E. Coessens, A. Ghysen, C. Dambly-Chaudiere, Smooth, a hnRNP encoding gene, controls axonal navigation in *Drosophila*, Genes Cells 10 (2005) 119–125.
[12] W. Rossoll, S. Jablonka, C. Andreassi, A.K. Kroning, K. Karle, U.R. Monani, M. Sendtner, Smn, the spinal muscular atrophy-determining gene product, modulates axon growth and localization of beta-actin mRNA in growth cones of motoneurons, J. Cell Biol. 163 (2003) 801–812.
[13] A.J. Hannan, P. Gunning, P.L. Jeffrey, R.P. Weinberger, Structural compartments within neurons: developmentally regulated organization of microfilament isoform mRNA and protein, Mol. Cell. Neurosci. 11 (1998) 289–304.
[14] J. Eberwine, K. Miyashiro, J.E. Kacharmina, C. Job, Local translation of classes of mRNAs that are targeted to neuronal dendrites, Proc. Natl. Acad. Sci. U. S. A. 98 (2001) 7080–7085.
[15] M. Yano, H.J. Okano, H. Okano, Involvement of Hu and heterogeneous nuclear ribonucleoprotein K in neuronal differentiation through p21 mRNA post-transcriptional regulation, J. Biol. Chem. 280 (2005) 12690–12699.
[16] R. Fujii, S. Okabe, T. Urushido, K. Inoue, A. Yoshimura, T. Tachibana, T. Nishikawa, G.G. Hicks, T. Takumi, The RNA binding protein TLS is translocated to dendritic spines by mGluR5 activation and regulates spine morphology, Curr. Biol. 15 (2005) 587–593.
[17] S. Huttelmaier, D. Zenklusen, M. Lederer, J. Dictenberg, M. Lorenz, X. Meng, G.J. Bassell, J. Condeelis, R.H. Singer, Spatial regulation of beta-actin translation by Src-dependent phosphorylation of ZBP1, Nature 438 (2005) 512–515.
[18] J. Condeelis, R.H. Singer, How and why does beta-actin mRNA target? Biol. Cell 97 (2005) 97–110.
[19] H.L. Zhang, R.H. Singer, G.J. Bassell, Neurotrophin regulation of beta-actin mRNA and protein localization within growth cones, J. Cell Biol. 147 (1999) 59–70.
[20] A.M. Krecic, M.S. Swanson, hnRNP complexes: composition, structure, and function, Curr. Opin. Cell Biol. 11 (1999) 363–371.
[21] W.M. Michael, Nucleocytoplasmic shuttling signals: two for the price of one, Trends Cell Biol. 10 (2000) 46–49.
[22] K. Kasashima, K. Terashima, K. Yamamoto, E. Sakashita, H. Sakamoto, Cytoplasmic localization is required for the mammalian ELAV-like protein HuD to induce neuronal differentiation, Genes Cells 4 (1999) 667–683.
[23] E.J. Wagner, M.A. Garcia-Blanco, Polypyrimidine tract binding protein antagonizes exon definition, Mol. Cell. Biol. 21 (2001) 3281–3288.
[24] V. Markovtsov, J.M. Nikolic, J.A. Goldman, C.W. Turck, M.Y. Chou, D.L. Black, Cooperative assembly of an hnRNP complex induced by a tissue-specific homolog of polypyrimidine tract binding protein, Mol. Cell. Biol. 20 (2000) 7463–7479.
[25] A.D. Polydorides, H.J. Okano, Y.Y.L. Yang, G. Stefani, R.B. Darnell, A brain-enriched polypyrimidine tract-binding protein antagonizes the ability of Nova to regulate neuron-specific alternative splicing, Proc. Natl. Acad. Sci. U. S. A. 97 (2000) 6350–6355.
[26] C. Gooding, P. Kemp, C.W. Smith, A novel polypyrimidine tract-binding protein paralog expressed in smooth muscle cells, J. Biol. Chem. 278 (2003) 15201–15207.
[27] M. Ichikawa, T. Kikuchi, H. Tateiwa, N. Gotoh, K. Ohta, J. Arai, N. Yoshimura, Role of PTB-like protein, a neuronal RNA-binding protein, during the differentiation of PC12 cells, J. Biochem. (Tokyo) 131 (2002) 861–868.
[28] T. Kikuchi, M. Ichikawa, J. Arai, H. Tateiwa, L. Fu, K. Higuchi, N. Yoshimura, Molecular cloning and characterization of a new neuron-specific homologue of rat polypyrimidine tract binding protein, J. Biochem. (Tokyo) 128 (2000) 811–821.
[29] A. Gil, P.A. Sharp, S.F. Jamison, M.A. Garcia-Blanco, Characterization of cDNAs encoding the polypyrimidine tract-binding protein, Genes Dev. 5 (1991) 1224–1236.
[30] F. Brunel, P.M. Alzari, P. Ferrara, M.M. Zakin, Cloning and sequencing of PYBP, a pyrimidine-rich specific single strand DNA-binding protein, Nucleic Acids Res. 19 (1991) 5237–5245.
[31] J.G. Patton, S.A. Mayer, P. Tempst, B. Nadal-Ginard, Characterization and molecular cloning of polypyrimidine tract-binding protein: a component of a complex necessary for pre-mRNA splicing, Genes Dev. 5 (1991) 1237–1251.
[32] A.L. Bothwell, D.W. Ballard, W.M. Philbrick, G. Lindwall, S.E. Maher, M.M. Bridgett, S.F. Jamison, M.A. Garcia-Blanco, Murine polypyrimidine tract binding protein. Purification, cloning, and mapping of the RNA binding domain, J. Biol. Chem. 266 (1991) 24657–24663.
[33] K. Lillevali, A. Kulla, T. Ord, Comparative expression analysis of the genes encoding polypyrimidine tract binding protein (PTB) and its neural homologue (brPTB) in prenatal and postnatal mouse brain, Mech. Dev. 101 (2001) 217–220.
[34] D.L. Black, Mechanisms of Alternative Pre-Messenger RNA Splicing, Annu. Rev. Biochem. 27 (2003) 27.
[35] C.A. Cote, D. Gautreau, J.M. Denegre, T.L. Kress, N.A. Terry, K.L. Mowry, A *Xenopus* protein related to hnRNP I has a role in cytoplasmic RNA localization, Mol. Cell 4 (1999) 431–437.
[36] A. Borman, M.T. Howell, J.G. Patton, R.J. Jackson, The involvement of a spliceosome component in internal initiation of human rhinovirus RNA translation, J. Gen. Virol. 74 (1993) 1775–1788.
[37] K.P. Knoch, H. Bergert, B. Borgonovo, H.D. Saeger, A. Altkruger, P. Verkade, M. Solimena, Polypyrimidine tract-binding protein promotes insulin secretory granule biogenesis, Nat. Cell Biol. 6 (2004) 207–214.
[38] P.A. Kosinski, J. Laughlin, K. Singh, L.R. Covey, A complex containing polypyrimidine tract-binding protein is involved in regulating the stability of CD40 ligand (CD154) mRNA, J. Immunol. 170 (2003) 979–988.
[39] K.G. Lassen, K.X. Ramyar, J.R. Bailey, Y. Zhou, R.F. Siliciano, Nuclear retention of multiply spliced HIV-1 RNA in resting CD4+ T cells, PLoS Pathog. 2 (2006) e68.
[40] R. Singh, J. Valcarcel, M.R. Green, Distinct binding specificities and functions of higher eukaryotic polypyrimidine tract-binding proteins, Science 268 (1995) 1173–1176.
[41] J. Xie, J.A. Lee, T.L. Kress, K.L. Mowry, D.L. Black, Protein kinase A phosphorylation modulates transport of the polypyrimidine tract-binding protein, Proc. Natl. Acad. Sci. U. S. A. 100 (2003) 8776–8781.
[42] I. Perez, J.G. McAfee, J.G. Patton, Multiple RRMs contribute to RNA binding specificity and affinity for polypyrimidine tract binding protein, Biochemistry 36 (1997) 11881–11890.
[43] M.G. Romanelli, F. Weighardt, G. Biamonti, S. Riva, C. Morandi, Sequence determinants for hnRNP I protein nuclear localization, Exp. Cell Res. 235 (1997) 300–304.
[44] M.G. Romanelli, C. Morandi, Importin alpha binds to an unusual bipartite nuclear localization signal in the heterogeneous ribonucleoprotein type I, Eur. J. Biochem. 269 (2002) 2727–2734.
[45] R.V. Kamath, D.J. Leary, S. Huang, Nucleocytoplasmic shuttling of polypyrimidine tract-binding protein is uncoupled from RNA export, Mol. Biol. Cell 12 (2001) 3808–3820.

[46] B. Li, T.S.B. Yen, Characterization of the nuclear export signal of polypyrimidine tract-binding protein, J. Biol. Chem. 277 (2002) 10306–10314.
[47] K.P. Knoch, R. Meisterfeld, S. Kersting, H. Bergert, A. Altkruger, C. Wegbrod, M. Jager, H.D. Saeger, M. Solimena, cAMP-dependent phosphorylation of PTB1 promotes the expression of insulin secretory granule proteins in beta cells, Cell. Metab. 3 (2006) 123–134.
[48] R.G. Fred, N. Welsh, Increased expression of polypyrimidine tract binding protein results in higher insulin mRNA levels, Biochem. Biophys. Res. Commun. 328 (2005) 38–42.
[49] L. Tillmar, N. Welsh, Glucose-induced binding of the polypyrimidine tract-binding protein (PTB) to the 3′-untranslated region of the insulin mRNA (ins-PRS) is inhibited by rapamycin, Mol. Cell. Biochem. 260 (2004) 85–90.
[50] R.E. Rydel, L.A. Greene, cAMP analogs promote survival and neurite outgrowth in cultures of rat sympathetic and sensory neurons independently of nerve growth factor, Proc. Natl. Acad. Sci. U. S. A. 85 (1988) 1257–1261.
[51] H.J. Song, M.M. Poo, Signal transduction underlying growth cone guidance by diffusible factors, Curr. Opin. Neurobiol. 9 (1999) 355–363.
[52] J. Qiu, D. Cai, M.T. Filbin, A role for cAMP in regeneration during development and after injury, Prog. Brain Res. 137 (2002) 381–387.
[53] W.D. Snider, F.Q. Zhou, J. Zhong, A. Markus, Signaling the pathway to regeneration, Neuron 35 (2002) 13–16.
[54] P.W. Gunning, G.E. Landreth, M.A. Bothwell, E.M. Shooter, Differential and synergistic actions of nerve growth factor and cyclic AMP in PC12 cells, J. Cell Biol. 89 (1981) 240–245.
[55] P.W. Gunning, P.C. Letourneau, G.E. Landreth, E.M. Shooter, The action of nerve growth factor and dibutyryl adenosine cyclic 3′:5′-monophosphate on rat pheochromocytoma reveals distinct stages in the mechanisms underlying neurite outgrowth, J. Neurosci. 1 (1981) 1085–1095.
[56] J.I. Nagy, J. Hacking, U.N. Frankenstein, E.A. Turley, Requirement of the hyaluronan receptor RHAMM in neurite extension and motility as demonstrated in primary neurons and neuronal cell lines, J. Neurosci. 15 (1995) 241–252.
[57] M.Y. Chou, J.G. Underwood, J. Nikolic, M.H. Luu, D.L. Black, Multisite RNA binding and release of polypyrimidine tract binding protein during the regulation of c-src neural-specific splicing, Mol. Cell 5 (2000) 949–957.
[58] B. Amir-Ahmady, P.L. Boutz, V. Markovtsov, M.L. Phillips, D.L. Black, Exon repression by polypyrimidine tract binding protein, RNA 11 (2005) 699–716.
[59] K.B. Seamon, W. Padgett, J.W. Daly, Forskolin: unique diterpene activator of adenylate cyclase in membranes and in intact cells, Proc. Natl. Acad. Sci. U. S. A. 78 (1981) 3363–3367.
[60] G.J. Hannon, J.J. Rossi, Unlocking the potential of the human genome with RNA interference, Nature 431 (2004) 371–378.
[61] N. Irwin, V. Baekelandt, L. Goritchenko, L.I. Benowitz, Identification of two proteins that bind to a pyrimidine-rich sequence in the 3′-untranslated region of GAP-43 mRNA, Nucleic Acids Res. 25 (1997) 1281–1288.
[62] J.C. Larcher, L. Gasmi, W. Viranaicken, B. Edde, R. Bernard, I. Ginzburg, P. Denoulet, Ilf3 and NF90 associate with the axonal targeting element of Tau mRNA, FASEB J. 18 (2004) 1761–1763.
[63] Y. Mori, K. Imaizumi, T. Katayama, T. Yoneda, M. Tohyama, Two cis-acting elements in the 3′ untranslated region of alpha-CaMKII regulate its dendritic targeting, Nat. Neurosci. 3 (2000) 1079–1084.
[64] E.H. Kislauskis, X. Zhu, R.H. Singer, Sequences responsible for intracellular localization of beta-actin messenger RNA also affect cell phenotype, J. Cell Biol. 127 (1994) 441–451.
[65] Y. Oleynikov, R.H. Singer, Real-time visualization of ZBP1 association with beta-actin mRNA during transcription and localization, Curr. Biol. 13 (2003) 199–207.
[66] A.F. Ross, Y. Oleynikov, E.H. Kislauskis, K.L. Taneja, R.H. Singer, Characterization of a beta-actin mRNA zipcode-binding protein, Mol. Cell. Biol. 17 (1997) 2158–2165.
[67] H. Lou, R.F. Gagel, S.M. Berget, An intron enhancer recognized by splicing factors activates polyadenylation, Genes Dev. 10 (1996) 208–219.
[68] P. Castelo-Branco, A. Furger, M. Wollerton, C. Smith, A. Moreira, N. Proudfoot, Polypyrimidine tract binding protein modulates efficiency of polyadenylation, Mol. Cell. Biol. 24 (2004) 4174–4183.
[69] C. Le Sommer, M. Lesimple, A. Mereau, S. Menoret, M.R. Allo, S. Hardy, PTB regulates the processing of a 3′-terminal exon by repressing both splicing and polyadenylation, Mol. Cell. Biol. 25 (2005) 9595–9607.
[70] A. Pautz, K. Linker, T. Hubrich, R. Korhonen, S. Altenhofer, H. Kleinert, The polypyrimidine tract binding protein (PTB) is involved in the post-transcriptional regulation of human iNOS expression, J. Biol. Chem. 281 (2006) 32294–32302.
[71] S.H. Back, Y.K. Kim, W.J. Kim, S. Cho, H.R. Oh, J.-E. Kim, S.K. Jang, Translation of polioviral mRNA is inhibited by cleavage of polypyrimidine tract-binding proteins executed by polioviral 3Cpro, J. Virol. 76 (2002) 2529–2542.
[72] M. Gama-Carvalho, N.L. Barbosa-Morais, A.S. Brodsky, P.A. Silver, M. Carmo-Fonseca, Genome wide identification of functionally distinct subsets of cellular mRNAs associated with two nucleocytoplasmic-shuttling mammalian splicing factors, Genome Biol. 7 (2006) R113.
[73] R. Reed, Coupling transcription, splicing and mRNA export, Curr. Opin. Cell Biol. 15 (2003) 326–331.
[74] D. Vaudry, P.J. Stork, P. Lazarovici, L.E. Eiden, Signaling pathways for PC12 cell differentiation: making the right connections, Science 296 (2002) 1648–1649.